

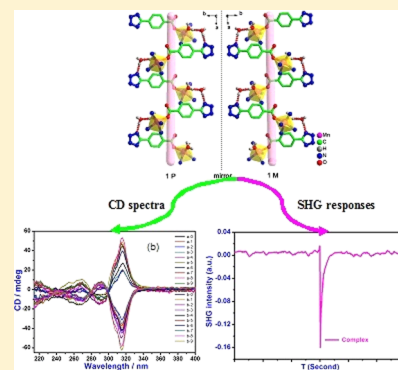
Supramolecular Interactions Induced Chirality Transmission, Second Harmonic Generation Responses, and Photoluminescent Property of a Pair of Enantiomers from in Situ [2 + 3] Cycloaddition Synthesis

Ji-Xing Gao, Jian-Bo Xiong, Qing Xu, Yu-Hui Tan, Yi Liu, He-Rui Wen, and Yun-Zhi Tang*

School of Metallurgy and Chemical Engineering, Jiangxi University of Science and Technology, Ganzhou, 341000, Jiangxi Province, P. R. China

Supporting Information

ABSTRACT: Spontaneous resolutions from an in situ reaction especially for a Sharpless reaction are really rare. Here we display a new pair of enantiomeric compounds Δ - and Λ -[Mn(4-tzba)(bpy)₂·H₂O](bpy)·3H₂O (labeled as Δ -1 and Λ -1 respectively) (4-tzba = 4-tetrazolbenzoic acid; bpy = 2,2'-bipyridine) from a Sharpless reaction. They crystallized in the *P*2₁2₁ chiral space group and demonstrated strong second harmonic generation (SHG) responses and red photoluminescence property. The chiral metal conformations were captured by the introduction of the distorted bpy and the in situ synthesized 4-tzba ligands. The hydrogen bonds connecting the 4-tzba and central metal play a crucial role in the chirality transmission, as well as the donor–acceptor type SHG nonlinear response.



INTRODUCTION

Chiral or non-centrosymmetric compounds are particularly interesting as their potential applications in the areas of information technology, optical storage, asymmetric catalysis, and chiral separation.^{1–6} Especially, second order nonlinear optical (NLO) materials have been receiving increasing attention because of their wide applications in areas including telecommunications, electric-optical devices, light modulators, and information storage. Traditionally, studies of second-order NLO materials were mainly focused on inorganic materials, such as quartz, potassium dihydrogen phosphate (KDP), lithium niobate (LiNbO₃), etc.^{1–11} However, they usually suffer a lot of drawbacks such as with low NLO responses, difficulty to synthesize, lack of optical quality, and slow electro-optic response times. Inorganic–organic hybrid materials have emerged in the past few years as promising candidates for NLO materials.^{1,12–15} These compounds usually combine high nonlinear optical coefficients of the organic molecules with excellent physical properties of the inorganic material. The coordination of organic ligands to metal ions can not only give rise to metal-to-ligand charge transfer transitions, but also allow the organic chromophores to be arranged in orderly geometries, enabling multidirectional charges transfer and exhibiting interesting photoluminescence properties.^{2,16}

However, the rational design and synthesis of inorganic–organic hybrid frameworks with chiral or acentric structures has proven to be a most challenging and laborious task because most hybrid frameworks are inclined to crystallize in a symmetric space group. It is well-known that three general methods are used to assemble homochiral complexes: (i) using

an enantio-pure ligand to translate the same handedness to the final framework; (ii) using a chiral precursors in the presence of chirality inducing agents such as chiral additives, chiral solvents, or chiral catalysts; (iii) spontaneous resolution during the crystallization from nonchiral starting materials.^{17–21} All three methods have their advantages and drawbacks; spontaneous resolution requires the generation of a chiral source which can transmit the stereochemical information. If there are preferential and extended homochiral interactions between a chiral source and its neighbors, the chirality would be able to extend to a higher dimensionality. The source of chirality may arise from the distorted coordination geometry of the central metals, the twisted conformation of the ligands, the supramolecular interactions, or a combination thereof; the targeted control of the resulting chirality is very difficult, and in some cases chiral agents are needed as reaction media, templates, or auxiliary ligands to induce chirality in the resulting structures.^{22–26}

It is inspiring that we recently synthesized the first enantiomers of metal tetrazole compound ([Cu(Tzmp)]_n, **2**) from in situ [2 + 3] cycloaddition reactions of a organic nitrile ligand with sodium azide in the presence of Cu²⁺ as a Lewis acid.²⁷ In **2**, the chirality originates in the chiral central copper atoms which is similar to the chiral carbon atoms in organic compounds. Tong et al. have discovered that axially chiral moieties of bpy can be isolated from the rotation of the two pyridine rings via spontaneous resolution.²⁸ As an ongoing

Received: November 28, 2015

Revised: January 13, 2016

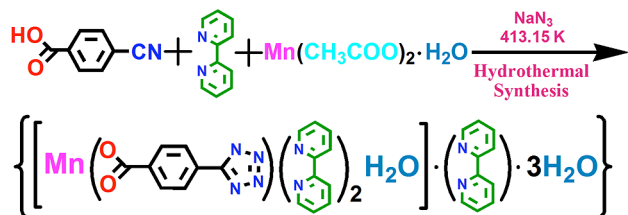
effect to obtain the homochiral compounds and analyze the mechanism of spontaneous resolution, we attempt to construct some new types of enantiomers from a [2 + 3] cycloaddition reaction by other supramolecular interactions.

Inspired by the previous work, we performed the Sharpless reaction of bpy, 4-tzba, sodium azide, and manganese acetate and obtained a new pair enantiomers from the [2 + 3] cycloaddition reaction. Here we detail their spontaneous resolution, crystal structures, circular dichroism (CD) spectra, second harmonic generation (SHG) responses, and photoluminescent properties.

EXPERIMENTAL SECTION

Synthesis. All reagents were purchased from commercial sources and used as received. Hydrothermal treatment of 4-tzba (0.0147 g, 0.1 mmol), NaN_3 (0.0195 g, 0.3 mmol) (Caution: Metal azides may be explosive), bpy (0.0468 g, 0.3 mmol), and $\text{Mn}(\text{CH}_3\text{COO})_2 \cdot \text{H}_2\text{O}$ (0.0382 g, 0.2 mmol) in a mixed solution of ethanol (0.5 mL) and water (2 mL) at 140 °C for 3 days give two different crystals: one is deep yellow block crystals (Δ -1), and the other (Λ -1) appears pale yellow with needle shapes (Figure S1 and Scheme 1). Yield: 0.0569 g,

Scheme 1. Preparation of Complex



72.6%, $\text{C}_{38}\text{H}_{36}\text{N}_{10}\text{O}_6\text{Mn}$ (783.71). Calcd for **1** (**1** = the mixture of Δ -1 and Λ -1): C, 58.24; H, 4.63; N, 17.87. Found: C, 58.32; H, 4.61; N, 17.79. IR (KBr, cm^{-1}): 3420(m), 1601(s), 1556(m), 1441(m), 1380(s), 1145(w), 1011(m), 758(s). Comparing the IR spectra of complex **1** and 4-tzba, a series of new strong peaks ranging from 1601 to 1441 cm^{-1} appear, while the absorption of cyano group at 2355 cm^{-1} $\text{Vas}(\text{C}\equiv\text{N})$ and $\text{Vs}(\text{C}\equiv\text{N})$ and the azide group in 2100 cm^{-1} disappear in **1** (Figure S2), indicating that the [2 + 3] Sharpless reaction between cyano group and azide anion has finished.^{10,29,30} The powder X-ray diffraction further conformed the phase purity (Figure S3).

Crystallography. We collected X-ray single-crystal diffraction data for Δ -1 and Λ -1 on a Bruker P4 diffractometer with $\text{Mo K}\alpha$ radiation ($\lambda = 0.71073 \text{ \AA}$) at 298 K using the θ -2 θ scan technique and corrected them by Lorentz–polarization and absorption corrections.^{31,32} Both crystal structures were solved by direct method and refined by the full-matrix method based on F^2 by means of the SHELXLTL software package.³³ Non-H atoms were refined anisotropically using all reflections with $I > 2\sigma(I)$. All H atoms were generated geometrically and refined using a “riding” model with $U_{\text{iso}} = 1.2U_{\text{eq}}$ (C). The small Flack parameters for Δ -1 (−0.009(8)) and Λ -1 (0.003(11)) clearly indicate that the absolute structure is correctly assigned in each case.³³ The asymmetric units and the packing views were drawn with DIAMOND (Brandenburg and Putz, 2005). Angles between some planes were calculated using DIAMOND, and other calculations were carried out using SHELXLTL. Crystal data and structures refinement for Δ -1 and Λ -1 are listed in Table 1. Their selected intra-atomic distances and bond angles are given in Table S1. Copies of this information can be obtained free of charge from The Director, CCDC, 12 Union Road, Cambridge, CB2 1EZ, UK. Fax (int. code) −44(1223)336−033 or E-mail: deposit@ccdc.cam.ac.uk or <http://www.ccdc.cam.ac.uk>. CCDC No. for Δ -1, 1438511 and for Λ -1, 1438510.

Physical Techniques. Elemental analyses (CHN) were carried out on a Vario EL III elemental analyzer. FT-IR spectra were recorded

Table 1. Crystal Data and Structure Refinement for Δ -1 and Λ -1

compound	Δ -1	Λ -1
empirical formula	$\text{C}_{38}\text{H}_{36}\text{MnN}_{10}\text{O}_6$	$\text{C}_{38}\text{H}_{36}\text{MnN}_{10}\text{O}_6$
formula weight	783.71	783.71
temperature (K)	293(2)	293(2)
crystal system	orthorhombic	orthorhombic
space group	$P2_12_12_1$	$P2_12_12_1$
<i>a</i> (Å)	10.9122(4)	10.9802(4)
<i>b</i> (Å)	14.8109(6)	14.8405(6)
<i>c</i> (Å)	23.2500(9)	23.2117(10)
<i>V</i> (Å ³)	3757.7(3)	3782.4(3)
μ (mm^{-1})	0.412	0.409
$D_{\text{calc}}/M \text{ gm}^{-3}$	1.385	1.376
<i>Z</i>	4	4
<i>F</i> (000)	1628	1628
Flack parameter	−0.009(8)	0.003(11)
GOF	1.010	1.005
R_1/wR_2 [$I > 2\sigma(I)$]	0.0511/0.0820	0.099/0.0813
$\Delta\rho_{\text{max}}/\Delta\rho_{\text{min}}$ ($\text{e}\cdot\text{\AA}^{-3}$)	0.832/−0.433	0.194/−0.259

from KBr pellets in the range of 400–4000 cm^{-1} on a Bruker TENSOR27 spectrometer. Powder X-ray diffraction patterns were recorded on a D8 ADVANCE diffractometer with $\text{Cu K}\alpha$ radiation at a scanning rate of 4° min^{-1} with 2θ ranging from 5° to 50° . PL emission spectra were measured at room temperature using a spectra fluorophotometer (JASCO, FP-6500) with a xenon lamp (150 W) as a light source. The solid state CD spectra were recorded on a Jasco-1500 circular dichroism spectropolarimeter at 293 K. The CD spectra were measured on the resulting complexes as crystals (ca. 0.4 mg) in 100 mg of oven-dried KBr. Spectra were recorded for the wavelength range 250–700 nm; for all the disks the path length was 0.3 mm. The SHG response was measured on powdered sample by using the experimental method adapted from that reported by the Kurtz–Perry method. An unexpanded laser beam with low divergence (pulsed Nd:YAG at a wavelength of 1064 nm, 5 ns pulse duration, 1.6 MW peak power, 10 Hz repetition rate) was used. The instrument model is FLS 920, Edinburgh Instruments, while the laser is Vibrant 355 II, OPOTEK.³⁴ Thermogravimetric analysis data were recorded on a PerkinElmer TGA 4000 instrument in the temperature range of 303–1073 °C under an N_2 atmosphere. Differential scanning calorimetry was carried out on a TA Q2000 DSC instrument in the temperature range 340–870 K under nitrogen at atmospheric pressure in aluminum crucibles with a heating rate of 10 K/min. The single-crystal samples with silver painted as the electrodes were used for dielectric studies, and dielectric permittivity ϵ ($\epsilon = \epsilon' - i\epsilon''$) was measured on a Tonghui TH2828A over the frequency range of 2 kHz to 1 MHz and in the temperature range from 170 to 340 K with the measuring *ac* voltage fixed at 1 V (a high voltage may puncture the samples).

RESULTS AND DISCUSSION

Crystal Structures. Single crystal X-ray diffraction analyses reveal that **1** contains Δ -1 and its enantiomorph Λ -1 with the same chiral space group of $P2_12_12_1$, suggesting that spontaneous resolution occurred. The Flack absolute structure parameters³³ (Table 1) further verify their chirality. As shown in Figure 1a, Δ -1 and Λ -1 have perfect mirror image; herein we only detailed the structure of Δ -1. The fundamental building unit of Δ -1 consists of one Mn(II) ion, one 4-(*SH*-tetrazol-5-yl)benzoic acid ligand, two coordinated bpy molecules, one lattice bpy molecule, one coordinated H_2O molecule, and three lattice H_2O molecules (Figure 1). The central Mn(II) adopts a hexa-coordinated octahedral geometry surrounded by four nitrogen atoms from two chelating bpy molecules, one oxygen

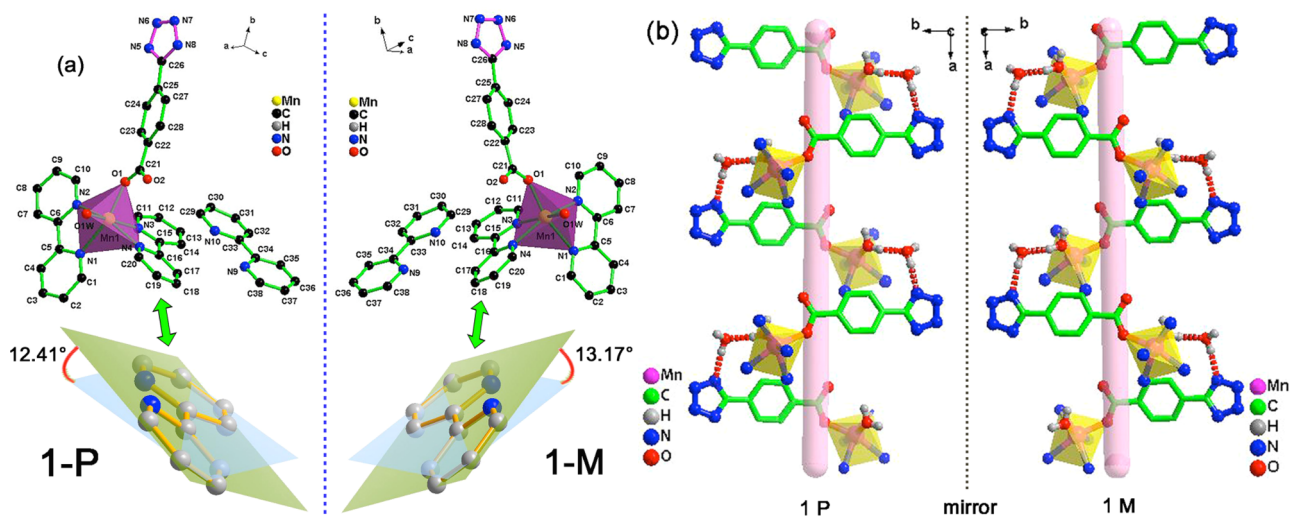


Figure 1. (a) View of the coordination environment of Mn(II) in Δ -1 (1-P, left) and Λ -1 (1-M, right) and the axially chiral conformations of bpy and the angle between two pyridine rings. (b) hydrogen-bonded right and left helix in Δ -1 and Λ -1.

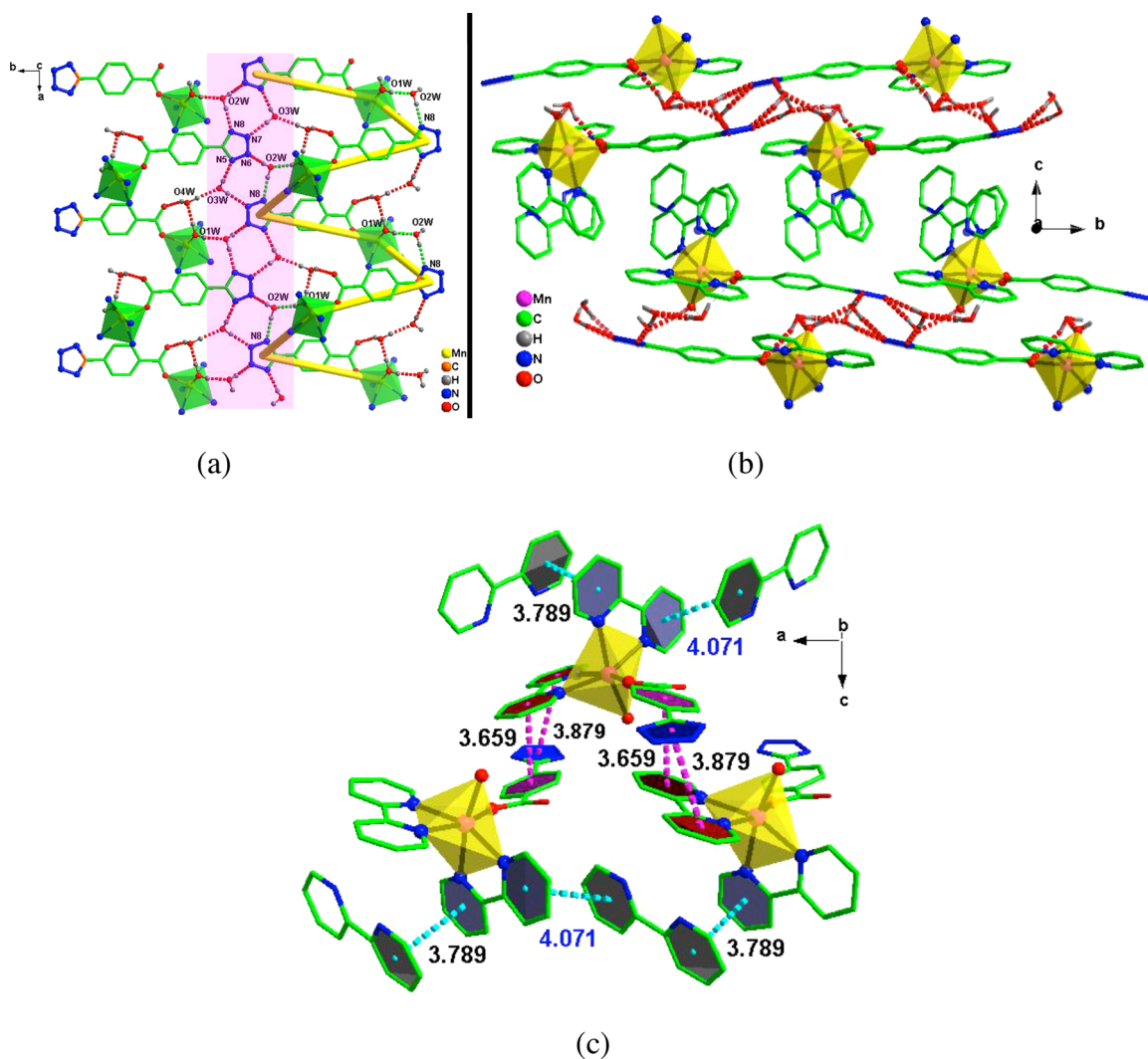


Figure 2. (a) View of the hydrophilic layer constructed by array of the tubular channels (pink area) and P helix in Δ -1. (b) Packing view along the *a*-axis and π - π interactions in Δ -1 (the red dashed line indicates hydrogen bonds). (c) π - π interactions between free bpy and coordinated bpy ligands.

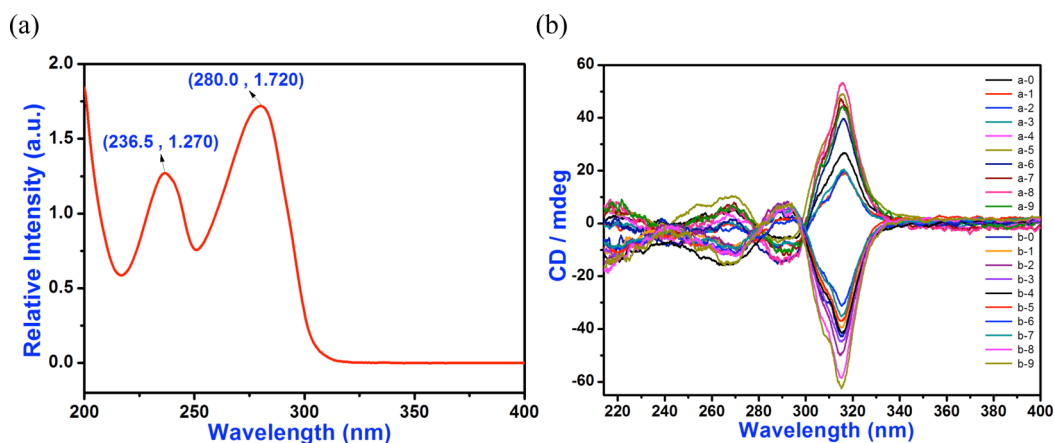


Figure 3. (a) Solid state UV absorption spectrum of **1**; (b) 10 groups of solid-state CD spectra of Δ -**1** and Λ -**1** show the opposite Cotton effects.

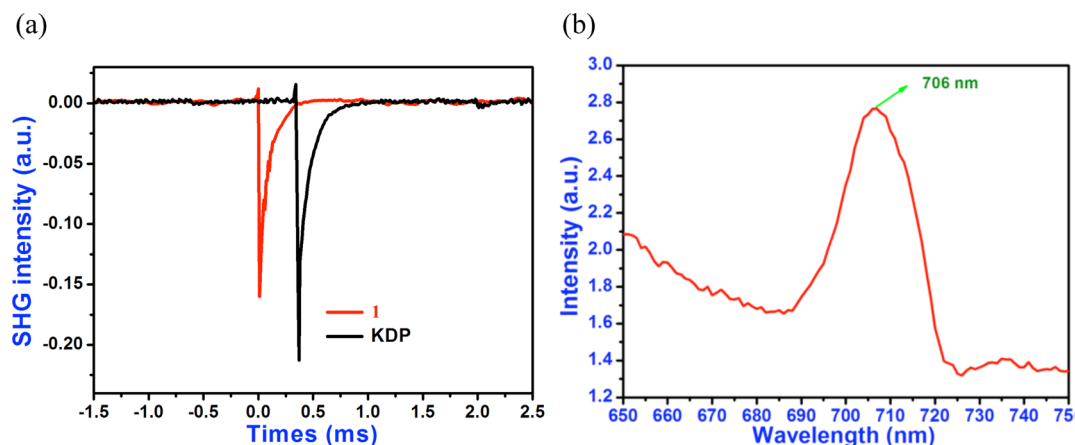


Figure 4. (a) Oscilloscope traces of SHG signals for the powder of **1** (b) solid state fluorescent emission spectrum.

atom from 4-tzba, and one coordinated water molecule, respectively. All the Mn–N and Mn–O distances ranged from 2.262(13) to 2.292(12) Å and 2.075(11) to 2.149(13) Å, respectively (Table S1), which are similar to the other analogous compounds.^{33,36} There are two chelating bpy molecules coordinated to the central metal; normally, bpy is achiral because of its rigid π – π conjugated structure between two pyridyl rings. However, it becomes an important element of chirality in **1**, in that the two axially chiral conformations of λ and δ are “locked”. The dihedral angle between two pyridyl planes is 12.41° (for Λ -**1** it is 13.17°) in one of the bpy, and the other one is still coplanar²⁸ (Figure 1b). In our previous work, we have reported other enantiomers of metal tetrazole compound ([Cu(Tzmp)]_n, **2**) from in situ [2 + 3] cycloaddition reactions;²⁷ however, they have totally different chiral sources. Complex **2**'s chirality comes from the chiral central copper atoms which can be viewed as the chiral carbon atoms in organic compounds, while compound **1**'s chirality originates from axially chiral conformations of bpy. As far as we know, although a lot of metal tetrazole complexes have been reported before, the spontaneous resolutions' cases from in situ [2 + 3] cycloaddition reactions are very rare.

Though the metal coordination number and coordination sphere geometry are crucial factors to generate chirality, another significant factor is an efficient transfer of chiral information from the achiral unit to a supramolecular structure through noncovalent interactions that simultaneously form homochiral helices.^{17–21,37–39} In Δ -**1**, the intermolecular

hydrogen bonds O(2W)–H(2WB)···N(8)#3 (2.785(2) Å) and O(1W)–H(1WB)···O(2W) (2.667(2) Å) (Table S2) combined with central metals to form an elegant right-handed P helix (for Λ -**1**, left-handed M helix) running along the 2₁ screw axis with the pitch equal to 10.91 Å (for Λ -**1**, 10.98 Å). The remarkable feature of P2₁2₁2₁ space group is the existence of 2₁ screw axes.²² The neighboring helices are fused side-by-side through H-bonds between the tetrazole rings and lattice water molecules (O(3W)–H(3WB)···N(7)#1, 2.873(2) Å and O(2W)–H(2WB)···N(8)#3, 2.785(2) Å) to form a layer parallel to the *ab* plane, generating chiral tubular channels running along the *a*-axis (Figure 2a). All in all, the hydrogen-bonding helices and channels formed the hydrophilic layer in the *ab* plane. The 2D sheets are further involved by π – π interactions to realize a 2D \rightarrow 3D antiparallel network along the *c*-axis, as depicted in Figure 2b. By virtue of the free bpy molecule, two π – π interactions are found with the distances being 3.789 and 4.071 Å (weak effect, Figure 2c), respectively. Thus, the lattice bpy molecule not only has a space-filling role in the material but also directs the formation of the whole framework. We have been unable to remove it without causing the structure to collapse. Generally speaking, the structural chirality of the central metals can be transferred to the whole polymeric framework via the supermolecular interactions.

To confirm the optical activity and enantiomeric nature of Δ -**1** and Λ -**1**, the solid-state CD spectra were recorded on their single crystals (Figure 3 and Figure S4). The UV absorption spectra of **1** in the region 236–280 nm showing two strong

peaks at 236 and 280 nm (Figure 3a) respectively are attributed to the d–d transition of Mn²⁺ ions and the ligand to metal charge transition (LMCT) in which the lone pair electrons of oxygen are transferred to the unoccupied d orbital of Mn²⁺ ions.^{40,41} The further experiment confirmed that the UV absorption peaks appear in the region 266 and 316 nm for bpy ligand and 298 and 362 nm for 4-tzba ligand respectively (Figure S5), far way from 236 and 280 nm. It should be noted that we have proven by experiment that the solid state UV absorption spectra of Δ -**1** and Λ -**1** are totally in line with that of **1**. Hence, the CD spectrum for Δ -**1** with yellow block morphology exhibits a negative Cotton effect at $\lambda_{\text{max}} = 315$ nm, indicating that the bulk sample is enantio enriched (Figure 3b).⁴² The origin of chirality of compound Δ -**1** should be closely related to the central chirality from the distortion of one chelating bpy molecule and the 2₁ screw axes with the same handedness assembled from the hydrogen bonds. In comparison, the CD spectrum of Λ -**1** with pale yellow and needle shapes shows the opposite CD signals at similar wavelengths.

Nonlinear Optical and Photoluminescence Properties.

A general method to judge whether compounds are non-centrosymmetric or homochiral is to measure their nonlinear optical properties. Thus, the solid-state SHG response of **1** was conducted at room temperature. As we expected, compound **1** shows a strong SHG signal (Figure 4a); the intensity (0.172) is close to (0.75 time) that of KDP (0.206) with the same test condition, indicating it may have potential applications in NLO materials. The reason may be attributed to the introduction of the distorted bpy and the in situ synthesized 4-tzba. Then, the hydrogen bonds connecting the 4-tzba and central metals play a crucial role in the donor–acceptor type SHG nonlinear response.

The solid-state luminescent emission spectra of **1** were studied at room temperature (Figure 4b). The emission peak at 706 nm under the excitation of 468 nm^{43–45} is produced by octahedrally coordinated manganese, and the emissive lifetime is 0.446 ms according to the fitted curve of **1** (Figure S6a). The emission at 706 nm is attributable to the $(t_{2g})^3(e_g)^2-(t_{2g})^4(e_g)^1$ electronic transition,^{43–45} since luminescent emission from ligand to ligand change transition of tetrazole complexes mainly occurs in the arrange of 400–550 nm (in our case, it is 513 nm, Figure S6b);^{46–48} meanwhile, the luminescent emission of bpy appears in 530 nm (Figure S6b). What is more, we have confirmed through experiment that the solid state fluorescent spectra of Δ -**1** and Λ -**1** are totally coincident with that of **1**. To the best of our knowledge, Mn²⁺ ions with the d⁵ electronic configuration have also been used to construct SHG-active materials. A donor–acceptor type of molecule often possesses both a large transition moment and a large excited state dipole moment; in **1**, the 4-tzba ligand can be regarded as a good donor- π -acceptor system (donor = tetrazole ring and acceptor = carboxylate group).^{1,30,49}

Thermogravimetric (TG), Differential Scanning Calorimetry (DSC), and Dielectric Behaviors. Weight loss along with a varied temperature can be demonstrated by TG analysis, a thermal signal from a structure phase transition can be detected by DSC measurements, and the dielectric constant (ϵ') abnormal originated from structural transition or composition loss can be captured by a temperature-dependent dielectric constant curve.^{50–54} Since **1**, Δ -**1**, and Λ -**1** have the same curves for their characterizations of TGA, DSC and dielectric constants. Here we just described the curves of **1** at length. As depicted in Figure 5, the first slope at 390 K with

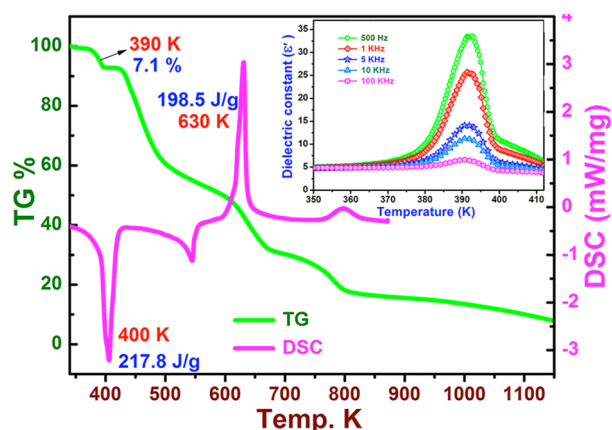


Figure 5. Thermogravimetric analyses (TGA) and DSC curves of **1**, inset: dielectric properties for **1** measured as a function of temperature under different frequencies.

7.1% weight loss was assigned to the removal of free water molecules (calcd. 6.9%) which identified well with the abnormal peak around 390 K of the dielectric constant. What is more, the dielectric constant peak values are frequency-dependent; the higher the frequency, the lower the dielectric constant. Interestingly, the DSC endothermic peak corresponding to the loss of free water molecules possesses a hysteresis of 10 K (400 K); this is because the successive endothermic process of leaving water molecules postponed the signal detection. The large endothermic value (217.8 J/g) in turn proved the strong hydrogen bonding effects of free water molecules. The successive three-step weight-loss (calcd. 86.1%) between 420 and 800 K indicates the structural decomposition and removal of the coordinated ligands were successive and synchronous. The distinct exothermic peak at 630 K should be attributed to the decomposition of tetrazole group, which can release lots of energy (198.5 J/g).^{55,56} The residue of the compound is calculated to be Mn (exper. 7.0%, calcd. 7.01%).

CONCLUSIONS

We have synthesized another new pair of enantiomeric tetrazole compounds by using in situ [2 + 3] cycloaddition. The chirality was captured by the coordination of the distorted bpy and further extended along the homochiral helices which are constructed from intermolecular hydrogen bonding. The CD spectrum study confirmed the spontaneous resolution process. The strong SHG response signal suggests they are possible potential NLO materials.

ASSOCIATED CONTENT

Supporting Information

The Supporting Information is available free of charge on the ACS Publications website at DOI: 10.1021/acs.cgd.5b01684.

IR spectra, illustration of crystals, powder X-ray diffraction patterns (PDF)

Accession Codes

CCDC 1438510–1438511 contain the supplementary crystallographic data for this paper. These data can be obtained free of charge via www.ccdc.cam.ac.uk/data_request/cif, or by emailing data_request@ccdc.cam.ac.uk, or by contacting The Cambridge Crystallographic Data Centre, 12, Union Road, Cambridge CB2 1EZ, UK; fax: +44 1223 336033.

AUTHOR INFORMATION

Corresponding Author

*E-mail: tangyunzhi75@163.com.

Notes

The authors declare no competing financial interest.

ACKNOWLEDGMENTS

This work was funded by the National Natural Science Foundation of China (Grant Nos. 21261009, 21471070 and 21461010), Young Scientist Foundation of Jiangxi Province and Jiangxi Province Science and Technology Support Program (20133BBE50020), and the Sustentation Fund of Education Department from Jiangxi Province (GJJ13434).

REFERENCES

- (1) Wang, C.; Zhang, T.; Lin, W. *Chem. Rev.* **2012**, *112*, 1084.
- (2) Tian, C.; Zhang, H.; Du, S. *CrystEngComm* **2014**, *16*, 4059.
- (3) Wei, Q.; Cheng, J. W.; He, C.; Yang, G. Y. *Inorg. Chem.* **2014**, *53*, 11757.
- (4) Zhong, D. C.; Meng, M.; Zhu, J.; Yang, G. Y.; Lu, T. B. *Chem. Commun.* **2010**, *46*, 4354.
- (5) Xu, Z. X.; Ma, Y. L.; Xiao, Y.; Zhang, L.; Zhang, J. *Cryst. Growth Des.* **2015**, *15*, 5901.
- (6) Tang, Y.-Z.; Yu, Y.-M.; Xiong, J.-B.; Tan, Y.-H.; Wen, H.-R. *J. Am. Chem. Soc.* **2015**, *137*, 13345.
- (7) Wei, L.; Wang, G. M.; He, H.; Yang, B. F.; Yang, G. Y. *Dalton Trans.* **2015**, *44*, 1420.
- (8) Zhao, S.; Gong, P.; Luo, S.; Bai, L.; Lin, Z.; Ji, C.; Chen, T.; Hong, M.; Luo, J. *J. Am. Chem. Soc.* **2014**, *136*, 8560.
- (9) Zhao, S.; Zhang, J.; Zhang, S.-Q.; Sun, Z.; Lin, Z.; Wu, Y.; Hong, M.; Luo, J. *Inorg. Chem.* **2014**, *53*, 2521.
- (10) Fu, D.-W.; Zhang, W.; Xiong, R.-G. *Cryst. Growth Des.* **2008**, *8*, 3461.
- (11) Sun, Z.-H.; Luo, J.-H.; Zhang, S.-Q.; Ji, C.-M.; Zhou, L.; Li, S.-H.; Deng, F.; Hong, M.-C. *Adv. Mater.* **2013**, *25*, 4159.
- (12) Li, L.; Ma, J.; Song, C.; Chen, T.; Sun, Z.; Wang, S.; Luo, J.; Hong, M. *Inorg. Chem.* **2012**, *51*, 2438.
- (13) Chen, N.; Li, M.-X.; Yang, P.; He, X.; Shao, M.; Zhu, S.-R. *Cryst. Growth Des.* **2013**, *13*, 2650.
- (14) Li, L.; Zhang, S.; Han, L.; Sun, Z.; Luo, J.; Hong, M. *Cryst. Growth Des.* **2013**, *13*, 106.
- (15) Zhao, S.-E.; Gong, P.-F.; Luo, S.-Y.; Liu, S.-J.; Li, L.-N.; Asghar, M. A.; Khan, T.; Hong, M.-C.; Lin, Z.-S.; Luo, J. H. *J. Am. Chem. Soc.* **2015**, *137*, 2207.
- (16) Wei, L.; Wang, G.-M.; He, H.; Yang, B.-F.; Yang, G.-Y. *Dalton Trans.* **2015**, *44*, 1420.
- (17) Perez-Garcia, L.; Amabilino, D. B. *Chem. Soc. Rev.* **2007**, *36*, 941.
- (18) Zhang, H.; Lin, P.; Shan, X.; Han, L.; Du, S. *CrystEngComm* **2014**, *16*, 1245.
- (19) Kang, Y.; Chen, S.; Wang, F.; Zhang, J.; Bu, X. *Chem. Commun.* **2011**, *47*, 4950.
- (20) Dura, G.; Carrión, M. C.; Jalón, F. A.; Rodríguez, A. M.; Manzano, B. R. *Cryst. Growth Des.* **2013**, *13*, 3275.
- (21) Bisht, K. K.; Suresh, E. *J. Am. Chem. Soc.* **2013**, *135*, 15690.
- (22) Liu, Q.-Y.; Wang, Y.-L.; Zhang, N.; Jiang, Y.-L.; Wei, J. J.; Luo, F. *Cryst. Growth Des.* **2011**, *11*, 3717.
- (23) Sun, J.-W.; Zhu, J.; Song, H.-F.; Li, G.-M.; Yao, X.; Yan, P.-F. *Cryst. Growth Des.* **2014**, *14*, 5356.
- (24) Kaur, A.; Hundal, G.; Hundal, M. S. *Cryst. Growth Des.* **2013**, *13*, 3996.
- (25) Gao, M.-J.; Yang, P.; Cai, B.; Dai, J.-W.; Wu, J.-Z.; Yu, Y. *CrystEngComm* **2012**, *14*, 1264.
- (26) An, G.; Yan, P.; Sun, J.; Li, Y.; Yao, X.; Li, G. *CrystEngComm* **2015**, *17*, 4421.
- (27) Tang, Y.-Z.; Xiong, J.-B.; Gao, J.-X.; Tan, Y.-H.; Xu, Q.; Wen, H.-R. *Inorg. Chem.* **2015**, *54*, 5462.
- (28) Liu, J.-L.; Bao, X.; Leng, J.-D.; Lin, Z.-J.; Tong, M.-L. *Cryst. Growth Des.* **2011**, *11*, 2398.
- (29) Tang, Y.-Z.; Zhou, M.; Huang, J.; Tan, Y.-H.; Wu, J.-S.; Wen, H.-R. *Inorg. Chem.* **2013**, *52*, 1679.
- (30) Ye, Q.; Li, Y.-H.; Song, Y.-M.; Huang, X.-F.; Xiong, R.-G.; Xue, Z. *Inorg. Chem.* **2005**, *44*, 3618.
- (31) Sheldrick, G. M. *SHELXS-97, Program for X-ray Crystal Structure Determination*; Universität of Göttingen: Göttingen, Germany, 1997.
- (32) Sheldrick, G. M. *SHELXS-97, Program for Crystal Structure Solution*; Universität of Göttingen: Göttingen, Germany, 1997.
- (33) Flack, H. D. *Acta Crystallogr., Sect. A: Found. Crystallogr.* **1983**, *39*, 876.
- (34) Kurtz, S. W.; Perry, T. T. *J. Appl. Phys.* **1968**, *39*, 3798.
- (35) Shi, G.; Shi, B.; Wang, Q.; Li, G. *Polyhedron* **2015**, *92*, 137.
- (36) Bhattacharya, S.; Bhattacharyya, A. J.; Natarajan, S. *Inorg. Chem.* **2015**, *54*, 1254.
- (37) Bisht, K. K.; Suresh, E. *Inorg. Chem.* **2012**, *51*, 9577.
- (38) Rao, A. S.; Pal, A.; Ghosh, R.; Das, S. K. *Inorg. Chem.* **2009**, *48*, 1802.
- (39) Matthew, D. G.; John, K. J.; Frank, J. L. *Cryst. Growth Des.* **2008**, *8*, 2899.
- (40) Yao, R.-X.; Cui, X.; Wang, J.; Zhang, X.-M. *Chem. Commun.* **2015**, *51*, 5108.
- (41) Rao, A. S.; Pal, A.; Ghosh, R.; Das, S. K. *Inorg. Chem.* **2009**, *48*, 1802.
- (42) Han, Q.; He, C.; Zhao, M.; Qi, B.; Niu, J.; Duan, C.-Y. *J. Am. Chem. Soc.* **2013**, *135*, 10186.
- (43) Zhang, Y.; Liao, W.-Q.; Fu, D.-W.; Ye, H.-Y.; Chen, Z.-N.; Xiong, R.-G. *J. Am. Chem. Soc.* **2015**, *137*, 4928.
- (44) Orgel, L. E. *J. Chem. Phys.* **1955**, *23*, 1958.
- (45) Orive, J.; Mesa, J. L.; Balda, R.; Fernández, J.; Rodríguez Fernández, J.; Rojo, T.; Arriortua, M. I. *Inorg. Chem.* **2011**, *50*, 12463.
- (46) Wei, Y.; Yu, Y.; Wu, K. *Cryst. Growth Des.* **2008**, *8*, 2087.
- (47) Baies, R.; Pralong, V.; Caignaert, V.; Saradhi, M. P.; Varadaraju, U. V.; Raveau, B. *Inorg. Chem.* **2008**, *47*, 6072.
- (48) Hu, Z.; Deibert, B. J.; Li, J. *Chem. Soc. Rev.* **2014**, *43*, 5815.
- (49) Li, Y.; Xu, G.; Zou, W.-Q.; Wang, M.-S.; Zheng, F.-K.; Wu, M.-F.; Zeng, H.-Y.; Guo, G.-C.; Huang, J.-S. *Inorg. Chem.* **2008**, *47*, 7945.
- (50) Zhang, W.; Ye, H.-Y.; Graf, R.; Spiess, H. W.; Yao, Y.-F.; Zhu, R.-Q.; Xiong, R.-G. *J. Am. Chem. Soc.* **2013**, *135*, 5230.
- (51) Maćzka, M.; Pietraszko, A.; Macalik, B.; Hermanowicz, K. *Inorg. Chem.* **2014**, *53*, 787.
- (52) Zhang, X.; Shao, X.-D.; Li, S.-C.; Cai, Y.; Yao, Y.-F.; Xiong, R.-G.; Zhang, W. *Chem. Commun.* **2015**, *51*, 4568.
- (53) Liao, W.-Q.; Zhang, Y.; Hu, C.-L.; Mao, J.-G.; Ye, H.-Y.; Li, P.-F.; Huang, S. D.; Xiong, R.-G. *Nat. Commun.* **2015**, *6*, 7338.
- (54) Sun, Z.-H.; Tang, Y.-Y.; Zhang, S.-Q.; Ji, C.-M.; Chen, T.-L.; Hong, M.-C.; Luo, J.-H. *Adv. Mater.* **2015**, *27*, 4795.
- (55) Kiselev, V. G.; Cheblakov, P. B.; Gritsan, N. P. *J. Phys. Chem. A* **2011**, *115*, 1743.
- (56) da Silva, G.; Bozzelli, J. W. *J. Org. Chem.* **2008**, *73*, 1343.